Structural disorganization and chain aggregation of high-amylose starch in different chloride salt solutions

Ying Li[†,‡,#], *Peng Liu*[*,†,‡,#], *Cong Ma*[†,‡], *Na Zhang*[†,‡], *Xiaoqin Shang*[†,‡], *Liming Wang*[†,‡], *Fengwei Xie,*[*,§,I]

[†]School of Chemistry and Chemical Engineering, and [‡]Fine Chemical Research Institute, Guangzhou University, 230 Wai Huan Xi Road, Guangzhou Higher Education Mega Center, Guangzhou, Guangdong 510006, China

[§]International Institute for Nanocomposites Manufacturing (IINM), WMG, University of Warwick, Coventry CV4 7AL, United Kingdom

[I]School of Chemical Engineering, The University of Queensland, Brisbane, Qld 4072, Australia

Corresponding Authors

[*] Email address: liu_peng@gzhu.edu.cn (P. Liu)

[*] Email address: f.xie@uq.edu.au; fwhsieh@gmail.com (F. Xie)

KEYWORDS: *High-amylose starch; Biopolymer; Metal chloride salt; Structural disorganization; Dissolution; Starch-metal ion coordinated complex; Nanoparticles; Rheology*

ABSTRACT: As high-amylose starch (HAS) has a higher content of linearly structured chains than other types of starch, it is more scientifically interesting to realize enhanced properties or new functions

for food and materials applications. However, the full dissolution of the compact granule structure of HAS is challenging under moderate conditions, which limits its applications. Here, we have revealed that the granule structure of HAS can be easily destructed by certain concentrations of acidic $ZnCl_2$, neutral $MgCl_2$ and alkaline $CaCl_2$ solutions (43 wt%, 34 wt%, and 31 wt%, respectively) at a moderate temperature (under 50 °C). The $ZnCl_2$ and $CaCl_2$ solutions resulted in complete dissolution of HAS granules, whereas small amounts of HAS granule remnants still existed in the $MgCl_2$ solution. The regenerated starch from the $CaCl_2$ solution was completely amorphous, that from the $ZnCl_2$ solution only presented a weak peak at 17°, and that from the $MgCl_2$ solution contained V-type crystallites. No new reflections were found on the FTIR spectra indicating all these three chloride solutions can be considered as a non-derivatizing solvent for starch. In all the three cases, nanoparticles were formed in the regenerated starch, which could be due to the aggregation of starch chains or their complexation with the metal cation. In addition, their water absorption ratio was 1.5 to 3 times that of the control (treated in water).

INTRODUCTION

Starch is a natural polymer formed by the photosynthesis in plants and is one of the major forms for plants to store energy. It is an abundant, cheap, renewable and environmentally-friendly resource.[1] Normal or wild-type starches consist of two types of glucose polymers, the predominately-linear amylose with rare branches, and the highly-branched amylopectin.[2] Amylose has a molecular mass of about 10^6 Daltons with long branches. Amylopectin contains a large number of short branches and is one of the largest biopolymers (about 10^8 Daltons).[3]

Starch with a higher content of amylose, compared to typical wild-type lines, can be termed as high-amylose starch (HAS). HAS can be biosynthesized in mutant cereal grains such as wheat, maize, rice, and barley and have some special properties such as heat resistance and digestion resistibility.[2] The granule structure of HAS has been extensively studied. Its inner region is composed of mainly loosely-packed amylopectin growth rings with semicrystalline lamellae,[4] while its compact periphery is supposed to be composed of entangled amylose chains.[5]

HAS has been used in many applications such as nutritional food, food processing, drug release, and biodegradable materials.[6] Due to the suitable molecular weight, linear molecular structure and densely populated hydroxyl groups, amylose has high chemical reactivity, which can be used to prepare modified starch,[7] starch-ion inclusion complexes[8] and starch-based materials.[9] However, the compact granule structure and the high gelatinization temperature of HAS limit its applications. As a result, how to destroy HAS granules and release starch chains is both scientifically and practically interesting.

Some solvents such as dimethyl sulfoxide (DMSO) and alkali solutions have been found to be capable of dissolving HAS. However, starch needs to be heated in 90% aqueous DMSO for about 24

h for the full dissolution; and alkaline solutions may induce depolymerization or oxidation of starch. Recent research has shown that ionic liquids (ILs) can dissolve starch and improve the degree of substitution (DS) and reaction efficiency for starch modification.[10] Some examples of these modified starch include acetylated starch,[11] cationic starch,[12] esterified starch,[13] carboxymethyl starch in 1-butyl-3-methylimidazolium chloride ([Bmim]Cl),[14] fatty-acid starch esters in 1-ethyl-3-methylimidazolium acetate ([Emim][OAc]),[15] and oxidized starch in a polyoxometalate IL.[16] However, the toxicity of ILs remains uncertain and their high prices also restrict their applications.[17]

Besides ILs, some inorganic salt solutions can also destruct starch granules.[18] Under certain concentrations, LiCl, KSCN, KI, BaF_2 and $BaBr_2$ solutions can be used to gelatinize starch granules at room temperature.[19] $ZnCl_2$ solution has been proved to be as an effective solvent for cassava starch[20] and a capable plasticizer and reinforcing agent for starch-based materials.[21] For the structural disorganization mechanism, Jane et al.[18] have indicated that, due to the electronegative nature of starch, anions tend to repel the ─OH groups of starch and stabilize starch granules; cations, on the other hand, attract the ─OH groups of starch and destabilize starch granules. However, Shimizu et al.[22] suggested that at high salt concentrations, the anion may enter the inside of the starch granule, breaking the granules and reducing the gelatinization temperature.

In this work, we compared the effects of $ZnCl_2$, $MgCl_2$ and $CaCl_2$ solutions, which are acid, neutral and alkaline solutions respectively, on the structural changes of HAS under a moderate temperature (50 °C). Based on that, we investigated the structural disorganization process of HAS granules and the aggregation of starch chains in the resulting salt solutions.

EXPERIMENTAL

Materials. Gelose 80 corn starch (G80) (about 80% amylose content, as determined by the manufacturer) was supplied by National Starch Pty Ltd. (Lane Cove, NSW 2066, Australia). Anhydrous zinc chloride ($ZnCl_2$), magnesium chloride ($MgCl_2$), and anhydrous calcium chloride ($CaCl_2$) were supplied by Aladdin Reagent (Shanghai) Co., Ltd. All these three chloride salts were chemically pure. Ethanol (analytical grade) was purchased from Guangzhou Chemical Reagent Factory (Guangzhou, China). All solutions were prepared with distilled water.

Sample Preparation. A certain amount of anhydrous $ZnCl_2$, $MgCl_2$ or $CaCl_2$ were added to the beaker to prepare 43 wt% $ZnCl_2$, 34 wt% $MgCl_2$ or 31 wt% $CaCl_2$ aqueous solutions (the concentrations were determined according to the discussion of Fig. 1). These salt solutions were then mixed with starch to achieve a starch concentration of 2 wt% (dry weight). After that, the solutions were located in a shaking bath at 50 °C. After a certain time, regenerated starch was obtained from the above solutions by adding absolute ethanol with continuous stirring (the volume of ethanol was about 2–5 times) and centrifuged under 3000 r/min for 5 min. Regenerated starch samples were washed three times by ethanol, and then dried and smashed into powder for further analysis. For comparison purposes, native G80 starch was also heated in a shaking bath at 50 °C for 4 h, which is taken as the control sample.

Light Microscopy. A polarized microscope (Axioskop 40 Pol/40A Pol, ZEISS) equipped with a 35mm SLA camera was used in the experimental work. The magnification used was 500× (50×10). Both normal and polarized lights were used for observation of starch suspensions (0.5 wt% concentration).

X-ray Diffraction (XRD). The crystallinity of starch samples was analyzed using an Xpert PRO diffractometer (PANalytical B.V., Netherlands) operated at 40 mA and 40 kV with Cu Kα radiation (wavelength 0.1542 nm). The scanning was performed from 5° to 50° 2θ at a speed of 10°/min and a step size of 0.033°. The degree of crystallinity (X_c) was estimated using MDI Jade 6 software according to a previous study.[23]

Fourier-Transform Infrared (FTIR). FTIR spectra in the range of 400–4000 cm^{-1} were obtained using a Bruker Tensor-27 FT-IR Spectrometer (Bruker, Billerica, MA, USA). The samples were mixed with KBr and well ground before being pressed into wafers.

Scanning Electron Microscopy (SEM). The morphology was imaged by a scanning electron microscope (JEOL JSM-7001F, Tokyo, Japan) with an accelerating voltage of 10 kV and a spot size of 6 nm. The samples were coated with platinum using an Eiko sputter coater.

Residual cations in regenerated starch. The amount of cation was detected by atomic absorption spectrometry (AAS, Thermo Scientific iCE 3500) and the sample preparation was followed by Chinese National Standards GB 5009.14-2017, GB 5009.92-2016, and GB 5009.241-2017. Specifically, 10 mL of 69 wt% hydrogen nitrate solution and 0.5 mL of 70 wt% perchloric acid solution were added to 5 g of the regenerated starch, and the obtained solution was heated to 220 °C for 2 h. After cooling, the volume of the solution was adjusted to 50 mL by distilled water, and the content of cation was detected using the AAS facility.

Intrinsic viscosity. Intrinsic viscosity was detected following a previous study.[20] Specifically, the samples were dispersed in 1M KOH solution and stirred in a boiling water bath for 10 min. The solutions were then cooled to room temperature and left overnight. After that, the solutions were

centrifuged under 3000 r/min for 6 min. The final concentrations of the solutions were 2.6–6.0 mg/mL. The intrinsic viscosity was measured by an Ubbelohde dilution capillary viscometer (size 37, Shanghai Liangjing Glass Instrument Factory, China), which was immersed in a water bath maintained at 30.0±0.1 °C. The efflux time of solvent and solutions were measured in triplicate and averaged. Then, intrinsic viscosity $[\eta]$ can be calculated using the equation:

$$[\eta] = \lim_{c \to 0} \frac{t - t_0}{c \times t_0} \qquad (1)$$

where t is the efflux time of the starch solution (s), t_0 is the efflux time of the KOH solution (s), and c represents the concentration of the starch solution (g/mL).

Water Absorption Measurement. The samples were soaked in water (5 wt% concentration) for 24 h and then vacuum filtrated. The water absorption was then calculated based on the weights before and after soaking. Triplicate tests were performed for each sample.

Rheology. After shaking at 50 °C for 4 h (see the section of Sample Preparation), the starch/chloride salt solutions were cooled to room temperature and tested immediately using a MCR 92 rheometer (Anton Paar GmbH, Austria) with a 60-mm-diameter cone-plate geometry and a Peltier temperature control system. For the salt solutions of different concentrations, the steady shear tests were carried out with the shear rate from 10 s^{-1} to 500 s^{-1} at 25 °C and 60 °C. Silicone oil (DC 200, Sigma–Aldrich) was placed around the edge of the measuring cell to maintain the moisture content of the sample. Silicone oil would hardly affect the experimental results, as it is immiscible with polysaccharide solutions and has a relatively lower viscosity (9.5 mPa/s at 20 °C). At least duplicate tests were performed for each sample.

The power-law model was used to describe the rheological behaviors:

$$\eta = K \cdot \dot{\gamma}^{n-1} \qquad (2)$$

where η is the viscosity (Pa·s) of the solution, $\dot{\gamma}$ is the shear rate (s^{-1}), K is the consistency (Pa·s), and n is the power-law index.

Statistical Analysis. Microsoft Excel software was used for regression fitting based on a modified power-law equation and obtaining the correlation coefficients (R^2). Data were analyzed based on one-way analysis of variance (ANOVA) and Duncan's test for a statistical significance of $p \leq 0.05$ using IBM SPSS Statistics software (v19.0).

RESULTS

Structural Disorganization of Starch in Chloride Salt Solutions. Fig. 1a shows the birefringence (Maltese cross) of G80 starch granules in $ZnCl_2$, $MgCl_2$, and $CaCl_2$ solutions at 50 °C for 4 h. Native G80 starch granules exhibited clear birefringence. The birefringence dimmed gradually with increasing salt concentration. When these salt solutions reached a certain concentration, namely 33% $ZnCl_2$, 27% $MgCl_2$ and 25% $CaCl_2$, the birefringence disappeared completely, suggesting the disruption of crystalline structure in the granules. However, as shown in the corresponding normal-light images, although some granules were swollen, most of them were still in their original shape. During the structural disorganization, their semicrystalline lamellae were destroyed by ions firstly, but their outer layer (which is formed by entangled amylose chains and is compact) could not be destroyed under these salt concentrations.[8] The remaining granule remnants were stable under these salt concentrations, even after 8 h of treatment.

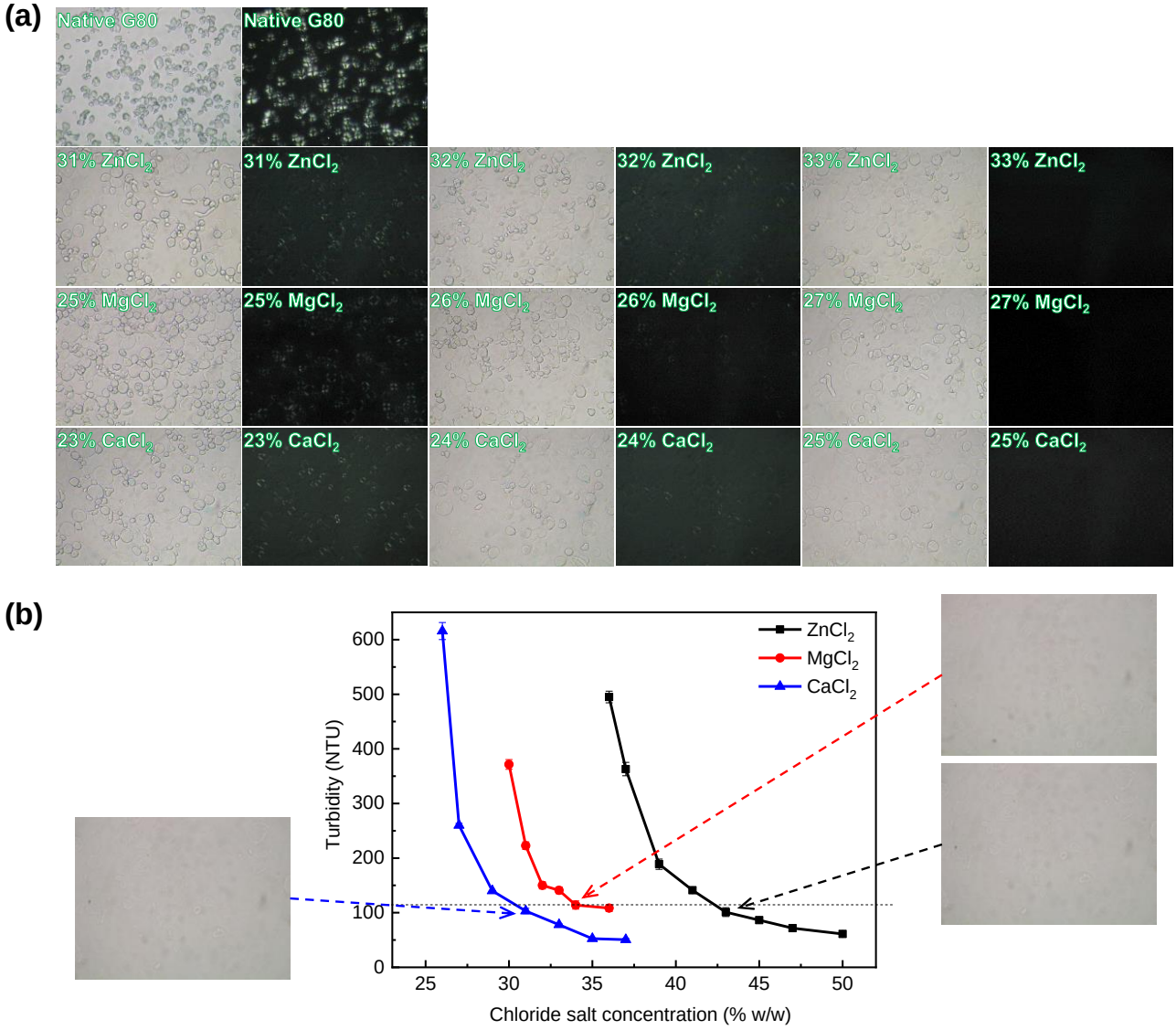

Fig. 1. (a) Microscopic images of G80 starch dissolved in chloride salt solutions under normal and polarized light; (b) Turbidity of G80 starch dissolved in three chloride salt solutions. The error bars represent standard deviations.

With increasing salt concentration, the birefringence of starch disappeared and the swollen granules became more and more ambiguous. The transparency of the solutions was characterized by turbidity (Fig. 1b). In previous studies,[17,20] when cassava starch was dissolved in $ZnCl_2$ solution with increasing concentration, there was an abrupt decrease in turbidity at a certain salt concentration (critical

concentration); after this point, the turbidity became stable. However, in this study, for G80 starch in $ZnCl_2$ and $CaCl_2$ solutions with increasing concentration, the turbidity kept decreasing. For the starch in $MgCl_2$ solution with increasing concentration, the turbidity was stable at around 110 NTU (36% is its saturated concentration under room temperature) and no obvious granules could be observed under microscopy. Thus, this value was considered as the threshold for a homogeneous solution.

Based on these results, the salt concentrations to destruct G80 starch were determined to be 43 wt% $ZnCl_2$, 34 wt% $MgCl_2$, and 31 wt% $CaCl_2$ (Table 1). Under these salt concentrations, the starch-salt solutions were transparent and all the granules vanished under microscopy. Table 1 listed the parameters for G80 starch to be destructed in three chloride salt solutions. The salt concentrations for the disappearance of both birefringence and granules follow the order of $ZnCl_2 > MgCl_2 > CaCl_2$.

Table 1. Parameters of G80 starch dissolved in three chloride salt solutions.

	$ZnCl_2$	$MgCl_2$	$CaCl_2$	Control
Salt concentration at birefringence disappearance (wt%)	33	27	25	–
pH of salt solution	4.21	7.10	9.52	–
Salt concentration at granule disappearance (wt%)	43	34	31	–
pH of salt solution	3.65	6.54	9.17	–
Content of cations in regenerated starch (mg/g)	53.0±1.3[a]	18.2±0.9	21.3±0.7	–
Water absorption ratio of regenerated starch (wt%)	152±9.6	222±8.7	144±12	60.9±5

[a] Average ± standard deviations.

Morphology of Regenerated Starch. Fig. 2 shows the SEM images of different regenerated starch samples and the control sample. The controlled samples displayed a nearly spherical shape with a smooth surface. For the regenerated starch from the $MgCl_2$ solution, the granules could be observed within 10 min of treatment; and after 30 min, some nanoparticles emerged on the surface of intact granules. After 4 h, some granules still remained with greater amounts of nanoparticles located on their surfaces. In other words, the $MgCl_2$ solution not only destructed the starch granules but also resulted in the formation of nanoparticles. The residual granules contributed to the high turbidity of the starch/$MgCl_2$ solution, which was stable at around 110 NUT (Fig. 1b).

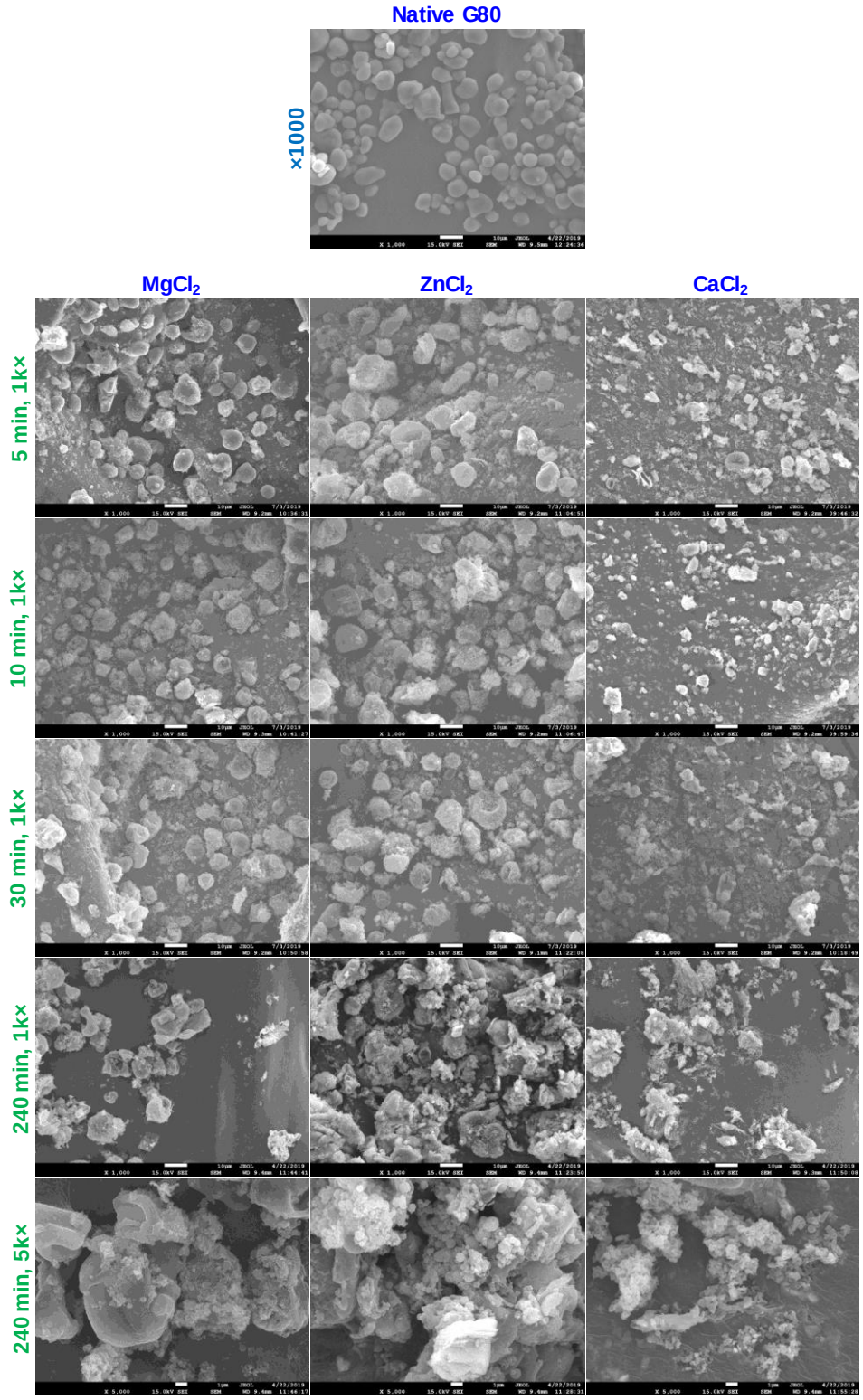

Fig. 2 Morphology of regenerated G80 starch from 34 wt% $MgCl_2$, 43 wt% $ZnCl_2$ and 31 wt% $CaCl_2$ solutions (magnification: 1k× or 5k×)

For the regenerated starch from the $ZnCl_2$ solution, 30 min of treatment led to some degree of

granule structural disorganization and the formation of nanoparticles. After 4 h, only nanoparticles (with some in the form of agglomerates) could be seen without original starch granules. For the regenerated starch from the $CaCl_2$ solution, all the starch granules changed into tiny fragments within 10 min. After 30 min, only agglomerated nanoparticles could be seen. This shows the efficient structural disorganization of G80 starch in the $CaCl_2$ solution.

Besides, we can see that the granules from the $MgCl_2$ and $ZnCl_2$ solutions within 10 min were larger than the controlled ones, which could be due to swelling. This result is in agreement with the microscopic observation (Fig. 1b) and with the previous results in hot water [24] and an IL.[25] However, after 30 min of treatment, the granules became smaller than the controlled ones due to the disintegration of granules.

Starch Structural Changes. Fig. 3 illustrates the XRD curves and the degree of crystallinity (X_c) of regenerated starch. For native G80 starch, the crystalline peaks located at 5.6°, 15°, 17°, 19.5°, 22° and 23.5° 2θ, which indicate the B-type pattern.[26-27] Its X_c was 14.7±0.2 %, similar to previous results.[21,28] For the regenerated starch from the $ZnCl_2$ solution (Fig. 3a), the crystalline pattern became very weak with only the reflection at 17° 2θ being apparent. For the samples from the $MgCl_2$ solution (Fig. 3b), only the peaks at 13° and 20° 2θ remained. These reflections are characteristic of the V-type crystalline pattern, which is due to the complexation of starch long chains with small molecules such as fat and iodine to form a single helical structure.[29] Besides, the peak in 17° 2θ remained within the first 5 min but disappeared after 10 min. For starch from the $CaCl_2$ solution (Fig. 3c), all peaks vanished within 5 min. The different crystalline patterns of regenerated starch show different interactions between starch chains and metal ions. Moreover, no new peaks emerged on the XRD curves, indicating

that the nanoparticles in the regenerated starch (Fig. 2) were not inorganic salt crystals.

Fig. 3d shows that in all these cases, X_c decreased sharply within 5 min. For the regenerated starch from $CaCl_2$ solution, X_c decreased to 0 within 5 min. For the samples from the $ZnCl_2$ and $MgCl_2$ solutions, X_c dropped sharply within 30 min, to 5.7±0.2 % and 10.2±0.2 % respectively. After that, the decrease in X_c was much slower. After 4 h of treatment, X_c was 3.6±0.3% and 7.3±0.3% for the samples in the $ZnCl_2$ and $MgCl_2$ solution respectively.

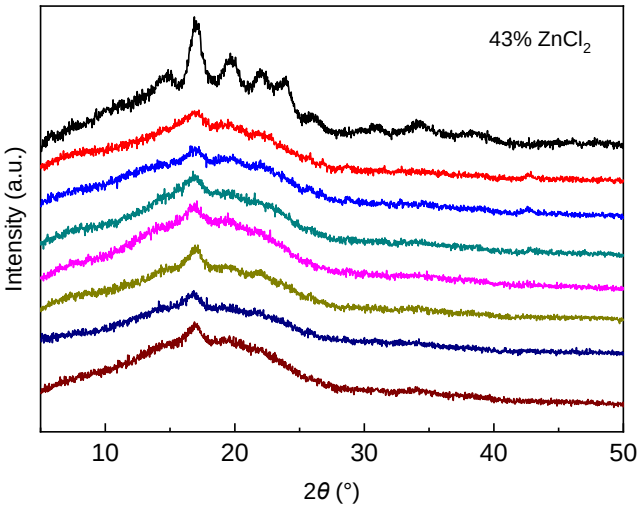

(a)

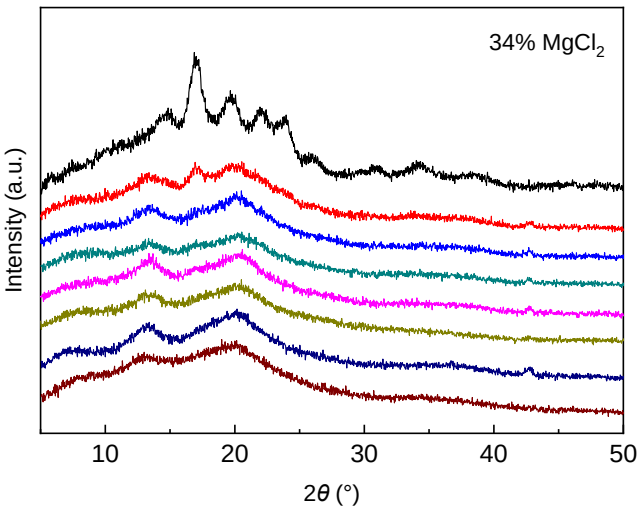

(b)

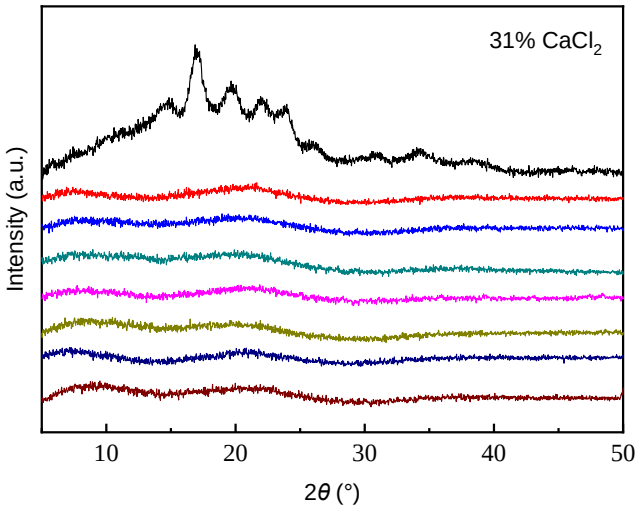

(c)

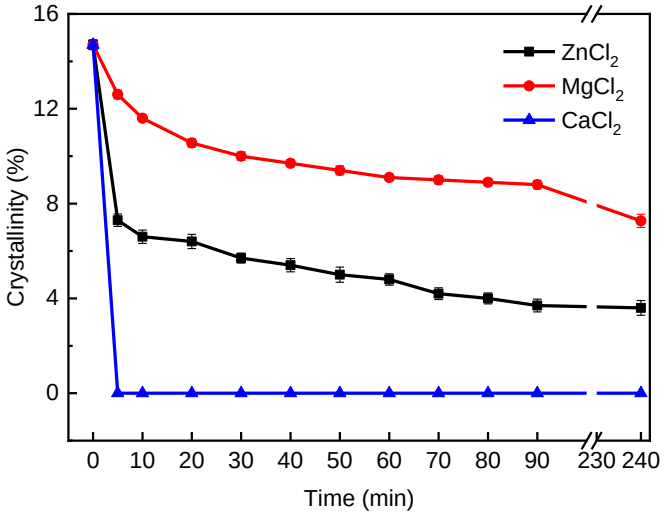

(d)

Fig. 3. XRD patterns for the regenerated G80 starch samples from 43 wt% $ZnCl_2$ (a), 34 wt% $MgCl_2$ (b), and 31 wt% $CaCl_2$ (c) solutions at different times of treatment (0 min, 5 min, 10 min, 20 min, 30 min, 60 min, 90 min and 240 min, from top to bottom). (d) shows the degree of crystallinity of the regenerated starch samples from 43 wt% $ZnCl_2$, 34 wt% $MgCl_2$, and 31 wt% $CaCl_2$ solutions as a function of time. The error bars represent standard deviations.

All FTIR spectra (Fig. 4) were similar without the appearance of new peaks, irrespective of native or regenerated starch samples, indicating no chemical changes in the regenerated starch. This is

different from previous studies,[20,30] where for cassava starch dissolved in a $ZnCl_2$ solution, the O—H bending of adsorbed water at 1647 cm^{-1} was shifted to 1627 cm^{-1}, indicating the water absorption function of the regenerated starch became weak. However, here for G80 starch, this shift was not apparent. Also, the water absorption ratios of the regenerated starch were much higher (nearly 1.5 to 3.5 times) than the controlled G80 starch (Table 1).

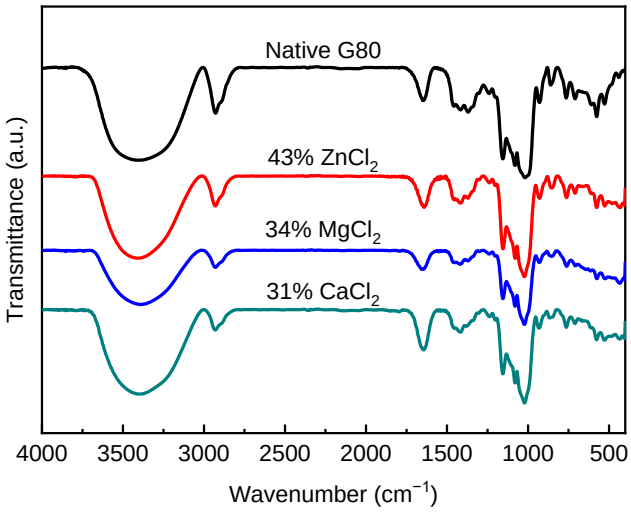

Fig. 4. FTIR spectra for native and regenerated G80 starch samples from 43 wt% $ZnCl_2$ solutions (a), 34 wt% $MgCl_2$ solutions (b), and 31 wt% $CaCl_2$ solutions (c) after 4 h of dissolution.

Intrinsic Viscosity of Regenerated Starch. Fig. 5 shows the intrinsic viscosity ([η]) of native and regenerated G80 starch. Intrinsic viscosity is an important parameter reflecting the size of a macromolecule in a given solvent at a certain temperature.[31] Native starch exhibited the highest [η] value. The sample from 34% $MgCl_2$ solution had a [η] value very close to that of native starch. The [η] value of regenerated starch from the $CaCl_2$ solution was higher than that from the $ZnCl_2$ solution, but both of them were significantly lower than that from the $MgCl_2$ solution.

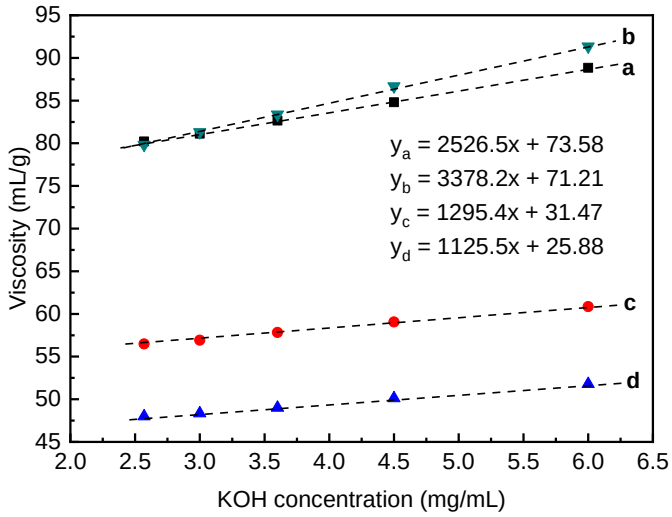

Fig. 5. Intrinsic viscosity of native starch (a), and regenerated starch samples from 34 wt% $MgCl_2$ solutions (b), 31 wt% $CaCl_2$ solutions (c), and 43 wt% $ZnCl_2$ solutions (d).

The intrinsic viscosity of polymers is caused by the friction force between the solvent and the solute in a dilute solution and can be used to reflect the size of the macromolecular conformation in the certain solution.[32-33] For starch, the size of their macromolecular conformation was caused by the degree of polymerization (DP), namely the molecular weight.[34] Therefore, a lower [η] value may indicate that the structural disorganization of starch granules in the $ZnCl_2$ and $CaCl_2$ solutions was accompanied by degradation, which was mainly caused by H^+ and OH^- ions. Moreover, since the pH value of 43 wt% $ZnCl_2$ solution was 3.65 and that of 31 wt% $CaCl_2$ solution was 9.17 (Table 1), the [η] value of the regenerated starch from the $ZnCl_2$ solution was lowest. The $MgCl_2$ solution is pH-neutral, so starch chains were hardly degraded, with similar [η] as that of native starch.

Since the degradation of molecular mass during the granule structural disorganization is mainly caused by the H^+ or OH^- ions in the solution, this kind of hydrolysis should have no selectivity on α-

(1-4) or α-(1-6) glycosidic bonds. In other words, chain degradation should occur to both amylose and amylopectin.

Rheological Properties of Starch/Chloride Salt Solutions. Since the concentration of saturated $MgCl_2$ solution at 25 °C is 36 wt% and the threshold concentration for $ZnCl_2$ solution to dissolve starch is 43 wt%, we compared the rheological properties of Gelose 80 starch in 34% $MgCl_2$ and 34% $CaCl_2$ solutions (Fig. 6a) and those of Gelose 80 starch in 43% $ZnCl_2$ and 43% $CaCl_2$ solutions (Fig. 6b). Fig. 6a shows that the viscosity of starch/$MgCl_2$ solution was higher than that of starch/$CaCl_2$ solution at 34% concentration. Fig. 6b shows that the viscosity of starch/$CaCl_2$ solution was higher than that of starch/$ZnCl_2$ solution at 43% concentration. Thus, the viscosity of different starch solutions should follow the order of $MgCl_2$ > $CaCl_2$ > $ZnCl_2$ under the same conditions.

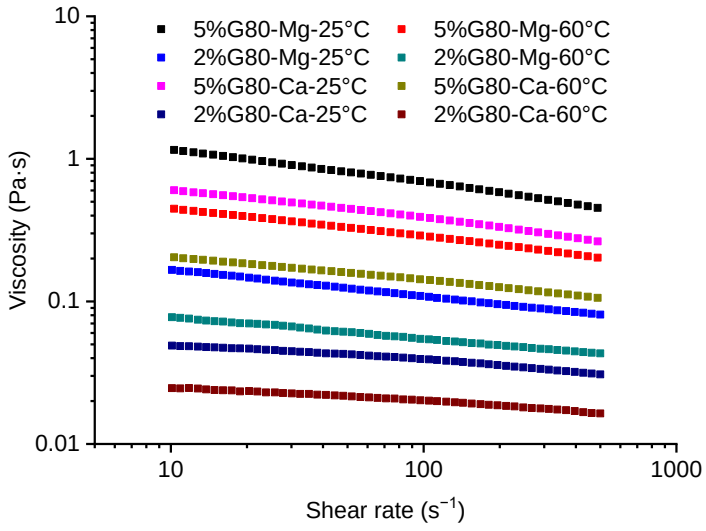

(a)

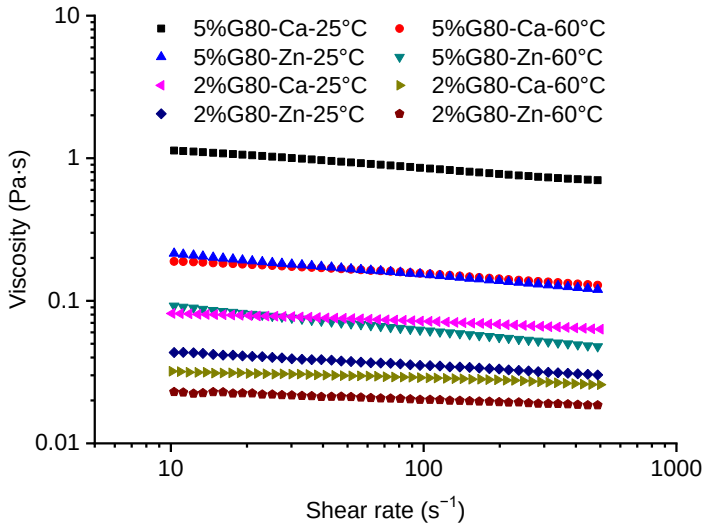

(b)

Fig. 6. Viscosity–shear rate curves for G80 starch in 34% $MgCl_2$ and $CaCl_2$ solutions (a) and in 43% $ZnCl_2$ and $CaCl_2$ solutions (b).

Table 2 shows the calculated parameters of the power-law equation at different temperatures and concentrations. Their correlation coefficients (R^2) were all higher than 0.99, showing a strong power-law dependence of viscosity on shear rate. The power-law index n for the starch/$MgCl_2$ solution is lower than that for the starch/$CaCl_2$ solution, and the n value of the starch/$CaCl_2$ solution is lower than that of the starch/$ZnCl_2$ solution. For a pseudo-plastic solution, a lower n value indicates a greater shear-thinning behavior and a larger molecular configuration of the solute.[35-37] Therefore, the n result reflects that the configuration of starch chains in the solutions followed the order of $MgCl_2$ > $CaCl_2$ > $ZnCl_2$, which is in agreement with the intrinsic viscosity results.

Table 2. Power-law parameters for starch in three chloride solutions

Sample	n	K	R^2

5%G80-34%$MgCl_2$-25°C	0.751[a]	2.1249[o]	0.9961[b]
5%G80-34%$MgCl_2$-60°C	0.791[c]	0.7438[k]	0.9972[c]
2%G80-34%$MgCl_2$-25°C	0.845[f]	0.1856[g]	0.9998[d]
2%G80-34%$MgCl_2$-60°C	0.888[g]	0.845[l]	0.9911[b]
5%G80-34%$CaCl_2$-25°C	0.76[b]	1.1732[m]	0.9967[b]
5%G80-34%$CaCl_2$-60°C	0.816[d]	0.3313[j]	0.9977[d]
2%G80-34%$CaCl_2$-25°C	0.88[g]	0.0771[d]	0.9955[b]
2%G80-34%$CaCl_2$-60°C	0.898[h]	0.0355[b]	0.9938[b]
5%G80-43%$ZnCl_2$-25°C	0.852[f]	0.3025[i]	0.999[d]
5%G80-43%$ZnCl_2$-60°C	0.835[e]	0.1329[f]	1[d]
2%G80-43%$ZnCl_2$-25°C	0.904[h]	0.0549[c]	0.9971[b]
2%G80-43%$ZnCl_2$-60°C	0.941[j]	0.0266[a]	0.9963[b]
5%G80-43%$CaCl_2$-25°C	0.875[g]	1.5158[n]	0.9925[b]
5%G80-43%$CaCl_2$-60°C	0.882[g]	0.2669[h]	0.9995[d]
2%G80-43%$CaCl_2$-25°C	0.923[i]	0.1026[e]	0.997[b]
2%G80-43%$CaCl_2$-60°C	0.934[j]	0.039[b]	0.9802[a]

Superscripts with different letters in the same column indicate significant differences ($p \leq 0.05$).

DISCUSSION

Structural disorganization Process of Starch in Chloride Salt Solutions. The structure of G80 granules includes the hilum locates in the center of granule, loosely-packed semicrystalline growth

rings around the hilum formed mainly by amylopectin, and a thick and compact outer layer formed primarily by entangled amylose chains.[5, 38-39]

The outer layer of starch granules exhibits a semipermeable-membrane-like behavior for both cations and anions, which prevents ions at low concentrations from entering the granule.[22] Since there are no cavities and channels on G80 granules,[40-41] the high salt concentration is needed for the penetration of ions through the outer layer. Once ions have passed through the outer layer and reached the hilum, they will destruct the semicrystalline lamellar regularity firstly, as reflected by the disappearance of birefringence and a significant reduction in X_c. The outer layer will require an even higher ion concentration to be disintegrated.

Aggregation of Starch Chains to Form Nanoparticles. Large amounts of nanoparticles can be seen in regenerated starch in all cases (see SEM results). These nanoparticles should not be the inorganic salt crystals (XRD results). Previous studies have shown that coordinated complexes may form between starch chains and some metal cations since the positively charged cations can be paired with the isolated charges on the oxygen atoms of starch hydroxyl groups.[42-45] Therefore, the nanoparticles observed could be considered as a form of starch–metal cation complexes, which can stabilize starch chains in the solution.

Moreover, different chloride salt solutions could result in different structures of starch–metal cation complex. The starch–Mg^{2+} complex presents a V-type crystalline structure. Regarding this, the coordination of Mg^{2+} with starch may allow the main chains of amylose or the long branches of starch macromolecules to form single helices, which then align into crystals under the neutral condition. However, such alignment may not be possible in the $ZnCl_2$ or $CaCl_2$ solution, where an acidic or

alkaline condition may restrict the formation of any crystalline structure. Therefore, starch–Zn^{2+} and starch–Ca^{2+} complexes are amorphous.

Early work has involved the preparation of starch–metal cation complexes, such as the bismuth (III) and bismuth (V) derivatives of starch,[46-47] starch–aluminum complex,[48] starch–copper complex and starch–iron complex.[49] These complexes are potential to be used in pharmaceutical applications such as for skin diseases, gastric ulcers, or hair growth. In this work, we have revealed a facile method to prepare starch–metal cation nanoparticles. The characteristics including embedding properties of these nanoparticles for active ingredients will be studied in the future.

Structural Disorganization Ability of Ions on Starch. Based on the residues and the degree of crystallinity, the structural disorganization ability of three chloride salt solutions on G80 starch granules follows the order of $CaCl_2$ > $ZnCl_2$ > $MgCl_2$. Then, what is the key factor to determine this ability?

For the structural disorganization mechanism of starch in ILs, previous studies have indicated that the anions have a protonation effect and can weaken the hydrogen bonding between starch chains, thus promoting the phase transition of granules.[50-51] Moreover, the cations can improve the protonation effect of anions by their ionic radius.[52-54] In other words, the larger the size of the cation, the stronger effect does the anion have. Moreover, besides the hydrogen-bonding capacity of IL anion, the viscosity of water/IL mixtures also plays a key role in the disruption of the starch structure.[55]

The three chloride salt solutions studies here present similar viscosities. The ionic radius of Ca^{2+} is 100 pm, that of Mg^{2+} is 72 pm, and that of Zn^{2+} is 74 pm,[56] which show no obvious difference as well. Therefore, the key factor should be attributed to the synergistic effect of ion. Specifically, based on the

acid–base proton theory, Cl^- may accept a proton and break the hydrogen bonds between starch chains; however, its protonation effect is very weak.[57] With the pH of these salt solutions noticed, it could be possible that H^+ and OH^- ions assist the structural disorganization.

For the alkaline $CaCl_2$ solution, both Cl^- and OH^- anions are strong hydrogen-acceptors.[58-59] Therefore, the structural disorganization ability of the $CaCl_2$ solution is the highest, and all residues changed into nanoparticles within a short time. When the acidic $ZnCl_2$ solution is used, the acid hydrolysis by H^+ facilitates the destruction of starch granules, accompanied by the degradation of starch chains. For $MgCl_2$ solution, which is pH-neutral, the concentration of H^+ and OH^- ions can be too low to facilitate the protonation by Cl^-, resulting in incomplete structural disorganization of starch granules (Fig. 7).

The threshold salt concentration to destruct starch granules follows the order of $CaCl_2$ < $MgCl_2$ < $ZnCl_2$. The reason should be the influence of H^+ or OH^- ions on the protonation effect of Cl^-. Specifically, OH^- anions can destroy the hydrogen bonds without varying the structural disorganization effect of Cl^-; thus, the threshold concentration of $CaCl_2$ solution is the lowest. However, although H^+ can hydrolyze starch chains, it hinders the protonation effect of Cl^- anions, as H^+ can accept the electron offered by Cl^-. Therefore, a greater number of Cl^- ions (a higher concentration of $ZnCl_2$) are needed to destruct starch granules.

Besides HAS, we found all these chloride salt solutions can fully destroy normal and waxy starch granules as well, and the dissolution of waxy and normal starches is easier than that of HAS, namely with lower salt concentrations and a shorter time. This may be explained by the looser granule structure of waxy and normal starches than that of HAS. The details regarding the dissolution of different

starches with different amylose contents by these chloride salt solutions will be discussed in our future work. Moreover, the dissolution mechanism is worth to be further investigated using theoretical chemistry approaches (e.g. molecular modelling simulations) and electrochemical studies.

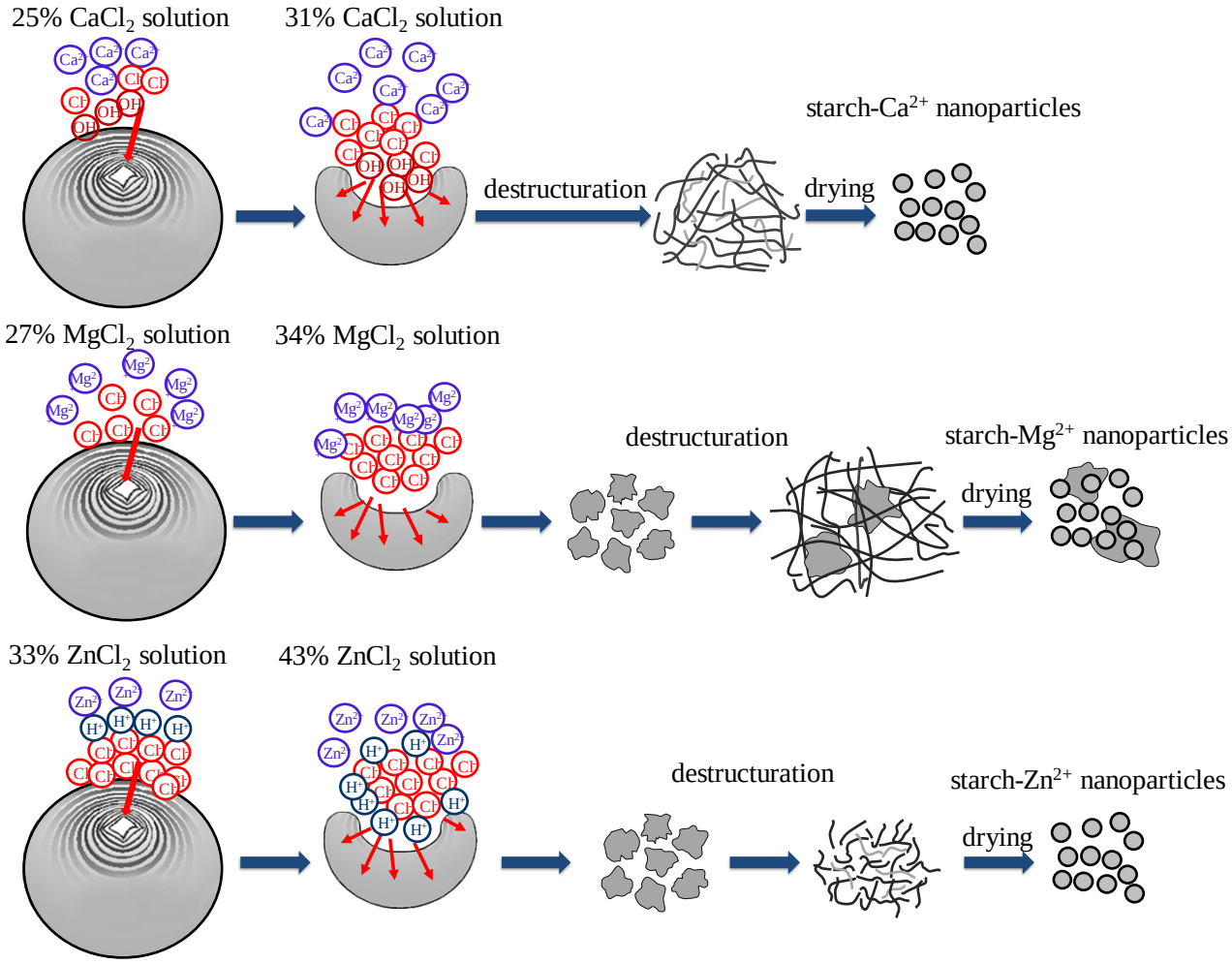

Fig. 7. Schematic diagram representing the structural disorganization of starch by metal chloride salt solutions.

CONCLUSIONS

Here, we have compared the effects of three chloride salt solutions on the structural disorganization of

G80 HAS granules. The crystalline structure of starch granules can be destroyed in 33 wt% $ZnCl_2$, 27 wt% $MgCl_2$, and 25 wt% $CaCl_2$ solutions, and the complete destruction of the granules needs 43 wt% $ZnCl_2$, 34 wt% $MgCl_2$, and 31 wt% $CaCl_2$ solutions at 50 °C. In other words, the threshold salt concentration follows the order of $CaCl_2 < MgCl_2 < ZnCl_2$. This should be mainly caused by the protonation effect of Cl^- anions on the hydrogen bonds, which is promoted by OH^- and hindered by H^+. Meanwhile, the degradation of starch by OH^- and H^+ is inevitable. The structural disorganization ability of the salt solutions follows the order of $CaCl_2 > ZnCl_2 > MgCl_2$. Specifically, starch chains dissociate in the $CaCl_2$ and $ZnCl_2$ solutions totally. Nevertheless, in $MgCl_2$ solutions, although most starch chains were detached, small amounts of granule residues remain.

Surprisingly, the regenerated starch from the chloride salt solutions is in the form of nanoparticles, which are likely to be formed by the complexation between the dissociated starch chains and the metal cations. XRD results indicate the different crystalline structures of these complexes, with Mg^{2+} cations promoting the formation of V-type crystallites whereas Ca^{2+} cations lead to completely amorphous nanoparticles. Besides, we also found that the water absorption ratio of regenerated starch is 1.5 to 3.5 times that of the control (treated in water). Thus, we demonstrate a facile method using non-derivatizing metal chloride salts to prepare absorbent biopolymer nanoparticles, which can be potentially used for the encapsulation and controlled release of active ingredients in food and pharmaceutical applications.

In all, this work has shown that HAS can be fully dissolved by cheap metal chloride salt solutions without derivatization effect. This finding could lead to ‘green’ processes for easy modification of HAS and for the preparation of plasticized starch-based ion-conductive materials.

AUTHOR INFORMATION

Corresponding Authors

* Email address: liu_peng@gzhu.edu.cn (P. Liu)

* Email address: f.xie@uq.edu.au; fwhsieh@gmail.com (F. Xie)

Author Contributions

P.L. and F.X. conceived and designed the study. Y.L. and C.M. conducted experiments and data analysis. The manuscript was written through the contributions of all authors. All authors have given approval to the final version of the manuscript. #These authors contributed equally.

Notes

The authors declare no competing financial interest.

ACKNOWLEDGMENT

This research was funded by the Natural Science Foundation of Guangdong Province (Project No. 2018A0303130048), the Pearl River S&T Nova Program of Guangzhou (Grant No. 201610010019), and the National Natural Science Foundation of China (NSFC) (Project No. 21106023) F. Xie acknowledges support from the European Union's Horizon 2020 research and innovation programme under the Marie Skłodowska-Curie grant agreement No. 798225. F. Xie also acknowledges support from the Guangxi Key Laboratory of Polysaccharide Materials and Modification, Guangxi University for Nationalities, China (Grant No. GXPSMM18ZD-02).

REFERENCES

(1) Haq, F.; Yu, H.; Wang, L.; Teng, L.; Haroon, M.; Khan, R. U.; Mehmood, S.; Ullah, R. S.; Khan, A.; Nazir, A. Advances in chemical modifications of starches and their applications. *Carbohydrate Research* **2019,** *476*, 12-35, DOI: 10.1016/j.carres.2019.02.007.

(2) Li, H.; Gidley, M. J.; Dhital, S. High-Amylose Starches to Bridge the "Fiber Gap": Development, Structure, and Nutritional Functionality. *Comprehensive Reviews in Food Science and Food Safety* **2019**, *18 (2)*, 362-379, DOI: 10.1111/1541-4337.12416.

(3) Vilaplana, F., Meng, D., Hasjim, J., Gilbert, R. G. Two-dimensional macromolecular distributions reveal detailed architectural features in high-amylose starches. *Carbohydrate Polymers* **2014**, *113*, 539-551, DOI: 10.1016/j.carbpol.2014.07.050.

(4) Yang, J.; Xie, F.; Wen, W.; Chen, L.; Shang, X.; Liu, P. Understanding the structural features of high-amylose maize starch through hydrothermal treatment. *International journal of biological macromolecules* **2016,** *84*, 268-274, DOI: 10.1016/j.ijbiomac.2015.12.033.

(5) Jane, J.-L. Current understanding on starch granule structures. *Journal of Applied Glycoscience* **2006**, *53(3)*, 205-213, DOI: 10.5458/jag.53.205.

(6) Benyerbah, N.; Ispas-Szabo, P.; Sakeer, K.; Chapdelaine, D.; Mateescu, M. A. Ampholytic and Polyelectrolytic Starch as Matrices for Controlled Drug Delivery. *Pharmaceutics* **2019,** *11* (6), 253, DOI: 10.3390/pharmaceutics11060253.

(7) Tang, H.; Fan, S.; Li, Y.; Dong, S. Amylose: Acetylation, Optimization, and Characterization. *J Food Sci* **2019,** *84* (4), 738-745, DOI: 10.1111/1750-3841.14487.

(8) Luo, Z.; Zou, J.; Chen, H.; Cheng, W.; Fu, X.; Xiao, Z. Synthesis and characterization of amylose-zinc inclusion complexes. *Carbohydr Polym* **2016,** *137*, 314-320, DOI: 10.1016/j.carbpol.2015.10.100.

(9) Li, M.; Liu, P.; Zou, W.; Yu, L.; Xie, F.; Pu, H.; Liu, H.; Chen, L. Extrusion processing and characterization of edible starch films with different amylose contents. *Journal of Food Engineering* **2011,** *106* (1), 95-101, DOI: 10.1016/j.jfoodeng.2011.04.021.

(10) Ren, F.; Wang, J.; Yu, J.; Xiang, F.; Wang, S.; Wang, S.; Copeland, L. Dissolution of Maize Starch in Aqueous Ionic Liquids: The Role of Alkyl Chain Length of Cation and Water:Ionic Liquid Ratio. *ACS Sustainable Chemistry & Engineering* **2019,** *7* (7), 6898-6905, DOI: 10.1021/acssuschemeng.8b06432.

(11) Biswas, A.; Shogren, R.; Stevenson, D.; Willett, J.; Bhowmik, P. K. Ionic liquids as solvents for biopolymers: Acylation of starch and zein protein. *Carbohydrate polymers* **2006,** *66* (4), 546-550, DOI: 10.1016/j.carbpol.2006.04.005.

(12) Wang, Y.; Xie, W. Synthesis of cationic starch with a high degree of substitution in an ionic liquid. *Carbohydrate Polymers* **2010,** *80* (4), 1172-1177, DOI: 10.1016/j.carbpol.2010.01.042.

(13) Zarski, A.; Ptak, S.; Siemion, P.; Kapusniak, J. Esterification of potato starch by a biocatalysed reaction in an ionic liquid. *Carbohydr Polym* **2016,** *137*, 657-663, DOI: 10.1016/j.carbpol.2015.11.029.

(14) Xie, W.; Zhang, Y.; Liu, Y. Homogenous carboxymethylation of starch using 1-butyl-3-methylimidazolium chloride ionic liquid medium as a solvent. *Carbohydrate polymers* **2011,** *85* (4), 792-797, DOI: 10.1016/j.carbpol.2011.03.047.

(15) Gao, J.; Luo, Z.-G.; Luo, F.-X. Ionic liquids as solvents for dissolution of corn starch and homogeneous synthesis of fatty-acid starch esters without catalysts. *Carbohydrate polymers* **2012,** *89* (4), 1215-1221, DOI: 10.1016/j.carbpol.2012.03.096.

(16) Chen, X.; Souvanhthong, B.; Wang, H.; Zheng, H.; Wang, X.; Huo, M. Polyoxometalate-based

ionic liquid as thermoregulated and environmentally friendly catalyst for starch oxidation. *Applied Catalysis B: Environmental* **2013,** *138*, 161-166, DOI: 10.1016/j.apcatb.2013.02.028.

(17) Chen, X.; Liu, P.; Shang, X.; Xie, F.; Jiang, H.; Wang, J. Investigation of rheological properties and conformation of cassava starch in zinc chloride solution. *Starch-Stärke* **2017,** *69* (9-10), 1600384, DOI: 10.1002/star.201600384.

(18) Jane, J. L. Mechanism of starch gelatinization in neutral salt solutions. *Starch-Stärke* **1993,** *45* (5), 161-166, DOI: 10.1002/star.19930450502.

(19) Lee, J. H.; You, S.; Kweon, D.-K.; Chung, H.-J.; Lim, S.-T. Dissolution behaviors of waxy maize amylopectin in aqueous-DMSO solutions containing NaCl and $CaCl_2$. *Food Hydrocolloids* **2014,** *35*, 115-121, DOI: 10.1016/j.foodhyd.2013.05.003.

(20) Lin, M.; Shang, X.; Liu, P.; Xie, F.; Chen, X.; Sun, Y.; Wan, J. Zinc chloride aqueous solution as a solvent for starch. *Carbohydrate polymers* **2016,** *136*, 266-273, DOI: 10.1016/j.carbpol.2015.09.007.

(21) Liu, P.; Li, Y.; Shang, X.; Xie, F. Starch-zinc complex and its reinforcement effect on starch-based materials. *Carbohydr Polym* **2019,** *206*, 528-538, DOI: 10.1016/j.carbpol.2018.11.034.

(22) Nicol, T. W. J.; Isobe, N.; Clark, J. H.; Matubayasi, N.; Shimizu, S. The mechanism of salt effects on starch gelatinization from a statistical thermodynamic perspective. *Food Hydrocolloids* **2019,** *87*, 593-601, DOI: 10.1016/j.foodhyd.2018.08.042.

(23) Liu, H.; Yu, L.; Simon, G.; Zhang, X.; Dean, K.; Chen, L. Effect of annealing and pressure on microstructure of cornstarches with different amylose/amylopectin ratios. *Carbohydr Res* **2009,** *344* (3), 350-354, DOI: 10.1016/j.carres.2008.11.014.

(24) Chen, P.; Yu, L.; Kealy, T.; Chen, L.; Li, L. Phase transition of starch granules observed by

microscope under shearless and shear conditions. *Carbohydrate Polymers* **2007,** *68* (3), 495-501, DOI: 10.1016/j.carbpol.2006.11.002.

(25) Mateyawa, S.; Xie, D. F.; Truss, R. W.; Halley, P. J.; Nicholson, T. M.; Shamshina, J. L.; Rogers, R. D.; Boehm, M. W.; McNally, T. Effect of the ionic liquid 1-ethyl-3-methylimidazolium acetate on the phase transition of starch: dissolution or gelatinization? *Carbohydr Polym* **2013,** *94* (1), 520-530, DOI: /10.1016/j.carbpol.2013.01.024.

(26) Cheetham, N. W. H.; Tao, L. Variation in crystalline type with amylose content in maize starch granules: an X-ray powder diffraction study. *Carbohydrate Polymers* **1998,** *36* (4), 277-284, DOI: 10.1016/S0144-8617(98)00007-1.

(27) Lopez-Rubio, A.; Flanagan, B. M.; Gilbert, E. P.; Gidley, M. J. A novel approach for calculating starch crystallinity and its correlation with double helix content: a combined XRD and NMR study. *Biopolymers* **2008,** *89* (9), 761-768, DOI: 10.1002/bip.21005.

(28) Chen, P.; Xie, F.; Zhao, L.; Qiao, Q.; Liu, X. Effect of acid hydrolysis on the multi-scale structure change of starch with different amylose content. *Food Hydrocolloids* **2017,** *69*, 359-368, DOI: 10.1016/j.foodhyd.2017.03.003.

(29) Kong, L.; Ziegler, G. R. Molecular encapsulation of ascorbyl palmitate in preformed V-type starch and amylose. *Carbohydrate Polymers* **2014,** *111*, 256-263, DOI: 10.1016/j.carbpol.2014.04.033.

(30) Vicentini, N.; Dupuy, N.; Leitzelman, M.; Cereda, M.; Sobral, P. Prediction of cassava starch edible film properties by chemometric analysis of infrared spectra. *Spectroscopy Letters* **2005,** *38* (6), 749-767, DOI: 10.1080/00387010500316080.

(31) Weiqing, L.; Tatiana, B. Dissolution of unmodified waxy starch in ionic liquid and solution

rheological properties. *Carbohydrate Polymers* **2013,** *93* (1), 199-206, DOI: 10.1016/j.carbpol.2012.01.090.

(32) Wolf, B. A. Polyelectrolytes Revisited: Reliable Determination of Intrinsic Viscosities. *Macromolecular Rapid Communications* **2007,** *28* (2), 164-170, DOI: 10.1002/marc.200600650.

(33) Botelho da Silva, S.; Krolicka, M.; van den Broek, L. A. M.; Frissen, A. E.; Boeriu, C. G. Water-soluble chitosan derivatives and pH-responsive hydrogels by selective C-6 oxidation mediated by TEMPO-laccase redox system. *Carbohydrate Polymers* **2018,** *186*, 299-309, DOI: 10.1016/j.carbpol.2018.01.050.

(34) Trinh, K. S.; Dang, T. B. Structural, physicochemical, and functional properties of electrolyzed cassava starch. *International journal of food science* **2019,** *2019*, 9290627, DOI: 10.1155/2019/9290627.

(35) Xie, F.; Yu, L.; Su, B.; Liu, P.; Wang, J.; Liu, H.; Chen, L. Rheological properties of starches with different amylose/amylopectin ratios. *Journal of Cereal Science* **2009,** *49*, 371-377, DOI: 10.1016/j.jcs.2009.01.002.

(36) Xie, F.; Pollet, E.; Halley, P. J.; Averous, L. Starch-based nano-biocomposites. *Progress in polymer science* **2013,** *38* (10-11), 1590-1628, DOI: 10.1016/j.progpolymsci.2013.05.002.

(37) Lancuški, A.; Vasilyev, G.; Putaux, J.-L.; Zussman, E. Rheological properties and electrospinnability of high-amylose starch in formic acid. *Biomacromolecules* **2015,** *16* (8), 2529-2536, DOI: 10.1021/acs.biomac.5b00817.

(38) Jiang, H.; Campbell, M.; Blanco, M.; Jane, J.-L. Characterization of maize amylose-extender (ae) mutant starches: Part II. Structures and properties of starch residues remaining after enzymatic

hydrolysis at boiling-water temperature. *Carbohydrate Polymers* **2010,** *80* (1), 1-12, DOI: 10.1016/j.carbpol.2009.10.060.

(39) Buléon, A.; Colonna, P.; Planchot, V.; Ball, S. Starch granules: structure and biosynthesis. *International journal of biological macromolecules* **1998,** *23* (2), 85-112, DOI: 10.1016/S0141-8130(98)00040-3.

(40) Chen, P.; Yu, L.; Simon, G. P.; Liu, X.; Dean, K.; Chen, L. Internal structures and phase-transitions of starch granules during gelatinization. *Carbohydrate Polymers* **2011,** *83* (4), 1975-1983, DOI: 10.1016/j.carbpol.2010.11.001.

(41) Chen, P.; Yu, L.; Chen, L.; Li, X. X. Morphology and microstructure of maize starches with different amylose/amylopectin content. *Starch-Starke* **2006,** *58* (12), 611-615, DOI: 10.1002/star.200500529.

(42) Tyrlik, S. K.; Tomasik, P.; Anderegg, J. W.; Baczkowicz, M. Titanium (IV) starch complexes. *Carbohydrate Polymers* **1997,** *34* (1), 1-7, DOI: 10.1016/S0144-8617(97)00102-1.

(43) Luo, Z.; Cheng, W.; Chen, H.; Fu, X.; Peng, X.; Luo, F.; Nie, L. Preparation and properties of enzyme-modified cassava starch-zinc complexes. *J Agric Food Chem* **2013,** *61* (19), 4631-4638, DOI: 10.1021/jf4016015.

(44) Wei, W.; Wu, S. Depolymerization of cellulose into high-value chemicals by using synergy of zinc chloride hydrate and sulfate ion promoted titania catalyst. *Bioresource Technology* **2017,** *241*, 760-766, DOI: 10.1016/j.biortech.2017.06.004.

(45) Szymońska, J.; Molenda, M.; Wieczorek, J. Study of quantitative interactions of potato and corn starch granules with ions in diluted solutions of heavy metal salts. *Carbohydrate Polymers* **2015,** *134*,

102-109, DOI: 10.1016/j.carbpol.2015.07.041.

(46) Bączkowicz, M.; Wójtowicz, D.; Anderegg, J. W.; Schilling, C. H.; Tomasik, P. Starch complexes with bismuth (III) and (V). *Carbohydrate Polymers* **2003,** *52* (3), 263-268, DOI: 10.1016/S0144-8617(02)00294-1.

(47) Yang, Y.; Ouyang, R.; Xu, L.; Guo, N.; Li, W.; Feng, K.; Ouyang, L.; Yang, Z.; Zhou, S.; Miao, Y. Review: Bismuth complexes: synthesis and applications in biomedicine. *Journal of Coordination Chemistry* **2015,** *68* (3), 379-397, DOI: 10.1080/00958972.2014.999672.

(48) Marusza, K.; Tomasik, P. Aluminium and arsenic(III) starchates. **1994,** *46* (1), 13-17, DOI: 10.1002/star.19940460105.

(49) Somsook, E.; Hinsin, D.; Buakhrong, P.; Teanchai, R.; Mophan, N.; Pohmakotr, M.; Shiowatana, J. Interactions between iron(III) and sucrose, dextran, or starch in complexes. *Carbohydrate Polymers* **2005,** *61* (3), 281-287, DOI: 10.1016/j.carbpol.2005.04.019.

(50) Jordan, T.; Schmidt, S.; Liebert, T.; Heinze, T. Molten imidazole – A starch solvent. *Green Chemistry* **2014,** *16* (4), 1967-1973, DOI: 10.1039/C3GC41818A.

(51) Sciarini, L.; Rolland-Sabaté, A.; Guilois, S.; Decaen, P.; Leroy, E.; Le Bail, P. Understanding the destructuration of starch in water–ionic liquid mixtures. *Green Chemistry* **2015,** *17* (1), 291-299, DOI: 10.1039/C4GC01248H.

(52) Ji, G.; Luo, Z.; Xiao, Z.; Peng, X. Synthesis of starch nanoparticles in a novel microemulsion with two ILs substituting two phases. *Journal of materials science* **2016,** *51* (15), 7085-7092, DOI: 10.1007/s10853-016-9952-1.

(53) Zhang, B.; Chen, L.; Xie, F.; Li, X.; Truss, R. W.; Halley, P. J.; Shamshina, J. L.; Rogers, R. D.;

McNally, T. Understanding the structural disorganization of starch in water–ionic liquid solutions. *Physical Chemistry Chemical Physics* **2015,** *17* (21), 13860-13871, DOI: 10.1039/C5CP01176K.

(54) Papanyan, Z.; Roth, C.; Wittler, K.; Reimann, S.; Ludwig, R. The dissolution of polyols in salt solutions and ionic liquids at molecular level: Ions, counter ions, and hofmeister effects. *ChemPhysChem* **2013,** *14* (16), 3667-3671, DOI: 10.1002/cphc.201300465.

(55) Ren, F.; Wang, J.; Luan, H.; Yu, J.; Copeland, L.; Wang, S.; Wang, S. Dissolution behavior of maize starch in aqueous ionic liquids: effect of anionic structure and water/ionic liquid ratio. *ACS Omega* **2019,** *4* (12), 14981-14986, DOI: 10.1021/acsomega.9b01768.

(56) Shannon, R. D., Revised effective ionic radii and systematic studies of interatomic distances in halides and chalcogenides. *Acta Crystallographica Section A* **1976**, *32* (5), 751-767, DOI: 10.1107/S0567739476001551.

(57) Chen, J.; Xie, F.; Li, X.; Chen, L. Ionic liquids for the preparation of biopolymer materials for drug/gene delivery: a review. *Green Chemistry* **2018,** *20* (18), 4169-4200 DOI: 10.1039/C8GC01120F.

(58) Dupont, J.; Suarez, P. A. Physico-chemical processes in imidazolium ionic liquids. *Physical Chemistry Chemical Physics* **2006,** *8* (21), 2441-2452, DOI: 10.1039/B602046A.

(59) Remsing, R. C.; Swatloski, R. P.; Rogers, R. D.; Moyna, G. Mechanism of cellulose dissolution in the ionic liquid 1-n-butyl-3-methylimidazolium chloride: a ^{13}C and $^{35/37}Cl$ NMR relaxation study on model systems. *Chemical Communications* **2006,** *2006* (12), 1271-1273, DOI: 10.1039/B600586C.

- For Table of Content Use Only -

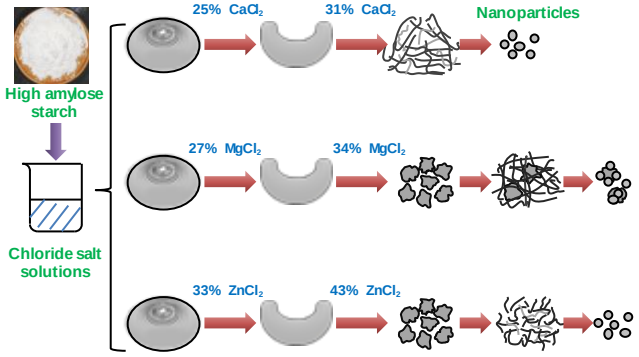

A facile method to prepare starch nanoparticles using cheap metal chloride salts is disclosed, leading to advanced applications of biopolymer.

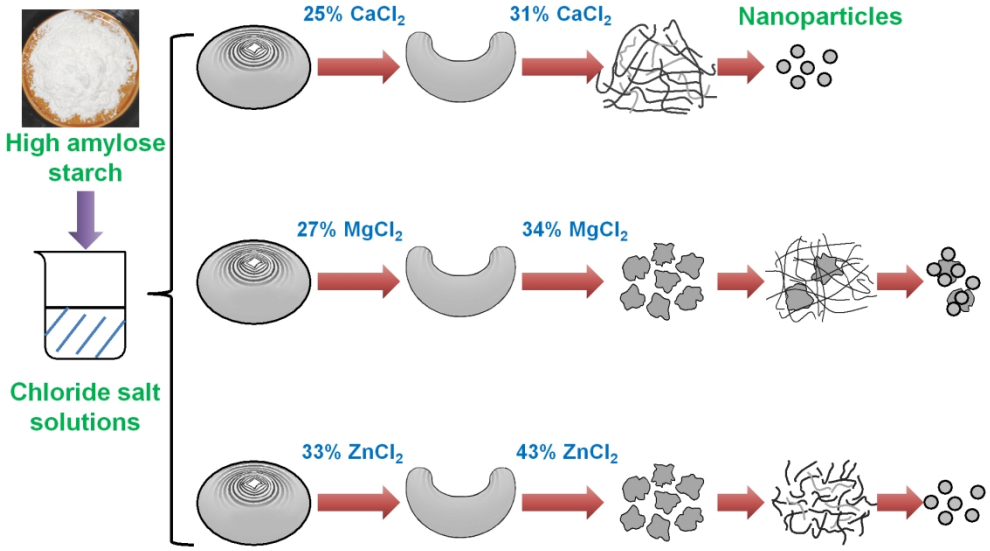

ToC graphic

532x297mm (96 x 96 DPI)